Quaternary Science Advances 14 (2024) 100174

Contents lists available at ScienceDirect

Quaternary Science Advances

journal homepage: www.sciencedirect.com/journal/quaternary-science-advances

Spatio-temporal variations of climate along possible African-Arabian routes of H. sapiens expansion

Markus L. Fischer [a,*], Philipp M. Munz [b], Asfawossen Asrat [c,d], Verena Foerster [e], Stefanie Kaboth-Bahr [f], Norbert Marwan [g], Frank Schaebitz [c], Wolfgang Schwanghart [h], Martin H. Trauth [a]

[a] University of Potsdam, Institute of Geosciences, Potsdam, Germany
[b] University of Tübingen, Department of Geosciences, Tübingen, Germany
[c] Botswana International University of Science and Technology, Department of Mining and Geological Engineering, Palapye, Botswana
[d] Addis Ababa University, School of Earth Sciences, Addis Ababa, Ethiopia
[e] University of Cologne, Institute of Geography Education, Cologne, Germany
[f] Free University Berlin, Institute of Geological Sciences, Berlin, Germany
[g] Potsdam Institute for Climate Impact Research, Potsdam, Germany
[h] University of Potsdam, Institute of Environmental Science and Geography, Potsdam, Germany

ARTICLE INFO

Keywords:
Eastern Africa
Arabia
Chew Bahir
Gulf of Aden
Pleistocene
Human evolution
Out-of-Africa migration
Linear time series analysis
Recurrence plots
Recurrence quantification analysis

ABSTRACT

Eastern Africa and Arabia were major hominin hotspots and critical crossroads for migrating towards Asia during the late Pleistocene. To decipher the role of spatiotemporal environmental change on human occupation and migration patterns, we remeasured the marine core from Meteor Site KL 15 in the Gulf of Aden and reanalyzed its data together with the aridity index from ICDP Site Chew Bahir in eastern Africa and the wet-dry index from ODP Site 967 in the eastern Mediterranean Sea using linear and nonlinear time series analysis. These analyses show major changes in the spatiotemporal paleoclimate dynamics at 400 and 150 ka BP (thousand years before 1950), presumably driven by changes in the amplitude of the orbital eccentricity. From 400 to 150 ka BP, eastern Africa and Arabia show synchronized wet-dry shifts, which changed drastically at 150 ka BP. After 150 ka BP, an overall trend to dry climate states is observable, and the hydroclimate dynamics between eastern Africa and Arabia are negatively correlated. Those spatio-temporal variations and interrelationships of climate potentially influenced the availability of spatial links for human expansion along those vertices. We observe positively correlated network links during the supposed out-of-Africa migration phases of *H. sapiens*. Furthermore, our data do not suggest hominin occupation phases during specific time intervals of humid or stable climates but provide evidence of the so far underestimated potential role of climate predictability as an important factor of hominin ecological competitiveness.

1. Introduction

For several decades, eastern Africa was considered the origin of *H. sapiens*, documented by the oldest fossil finds from Omo Kibish (233 ± 22 ka BP, McDougall et al., 2005; Vidal et al., 2022) and Herto (160–154 ka BP, White et al., 2003), from where our direct ancestors are thought to have spread across the rest of the continent and beyond. However, recent finds of human fossils, related stone tools and in several parts of Africa between roughly 315 and 75 ka ago, i.e., northwest Africa at Jebel Irhoud (Hublin et al., 2017), eastern Africa (Roberts et al., 2020), southern Africa (Chan et al., 2019) and more recently Arabia (Groucutt et al., 2021; Bretzke et al., 2022) initiated a lively discussion on a pan African structured population model of the origin, evolution, and spread of *H. sapiens* (Scerri et al., 2018, 2019; Bergström et al., 2021).

The Arabian peninsula is hereby a key region of hominin expansion, occupation, and a major network vertex (occupation hotspot) that connected African and Eurasian hominin groups during less arid phases of the late Pleistocene (Gebregiorgis et al., 2021). This region may have been the primary crossroad for the hominin *out of Africa* dispersal by

* Corresponding author.
E-mail address: markus.lothar.fischer@uni-potsdam.de (M.L. Fischer).

https://doi.org/10.1016/j.qsa.2024.100174
Received 2 November 2023; Received in revised form 20 February 2024; Accepted 27 February 2024
Available online 8 March 2024

either the northern route, the Nile-Levantine corridor (Breeze et al., 2016), or the southern route, the Strait of Bab-al-Mandab (Armitage et al., 2011). At times, *windows of opportunity* (Rosenberg et al., 2011; Ao et al., 2024) with favorable conditions may have enabled demographic expansion, occupation, and the activation of Arabia as a hominin hotspot and African-Eurasian crossroad (Parton et al., 2015; Beyer et al., 2021; Scerri et al., 2021). Nevertheless, in the context of expansion and migratory movements, the debate continues as to whether it was more humid (e.g., Trauth et al., 2005; Castañeda et al., 2009; Asrat et al., 2018) or dry conditions (e.g., Carto et al., 2009; Stewart and Fenberg, 2018), or a spatio-temporal complex pattern of both (e.g., Trauth et al., 2010; Timmermann and Friedrich, 2016; Tierney et al., 2017; Kaboth-Bahr et al., 2021; Schaebitz et al., 2021; Foerster et al., 2022), that favored human mobilization and expansion.

The causes of climate change in eastern Africa including the spatio-temporal differences are largely understood. In this context, it is considered certain that solar radiation in the lower latitudes controls the intensity of the African-Asian monsoon on orbital time scales (Trauth et al., 2003; Kutzbach et al., 2020). This fundamental mechanism is superimposed by the influence of sea-surface temperatures (and their El Niño-Southern Oscillation and Indian Ocean Dipole related anomalies) of the neighboring oceans (e.g., Kaboth-Bahr et al., 2021; Palmer et al., 2023). The importance of atmospheric greenhouse gas concentrations and, even more, the influence of northern ice sheets, however, is passionately debated (e.g., Otto-Bliesner et al., 2014; Beck et al., 2018; Kutzbach et al., 2020; Trauth et al., 2021a; Gosling et al., 2022). Here, well-known connections between external forcing and regional vs. local response of environmental conditions still encounter a distinct Amero-Eurocentric perspective of glacial-interglacial forcing of low latitude climate with respective *windows of opportunity* for human occupation (Bretzke et al., 2022).

Whatever the causes, the currently available climate data suggest that favorable living conditions for humans did not prevail concurrently (e.g., Nicholson et al., 2020; Foerster et al., 2022; Trauth et al., 2021b; Kaboth-Bahr et al., 2021). A predominantly linear response of regional climate to orbital forcing is modulated by nonlinear vegetation feedback (Claussen and Gayler, 1997;Fischer et al., 2021), an amplification effect due to the local topography (Trauth et al., 2010), orographic vegetation displacement (Coetzee, 1964), and nonlinear states of atmospheric circulation (Palmer et al., 2023). A lack of chronologically continuous and well-resolved paleoclimate records of Arabia and, until recently, of eastern Africa has led to a gap in profound paleoclimate dynamic comparisons between these major hominin sub-regions. For instance, the unstable political situation in the region, namely widespread piracy in the Arabian Sea, the Red Sea, and the Gulf of Aden, has largely prevented deep-sea drilling over the past three decades. Therefore, paleoclimate research in the region is largely based on old core material from the 1970s and 1980s.

Here we present new data and analyses of such a core from the Gulf of Aden, the R/V Meteor core KL 15 collected in 1987, compared with the lacustrine record of eastern African climate from ICDP Site Chew Bahir (Foerster et al., 2022) and the northern African wetness index from ODP Site 967 (e.g., Grant et al., 2017) (Fig. 1). First, these three records are analyzed for correlation on orbital and millennial time scales to test the null hypothesis that changes have the same temporal sign and a similar magnitude. We then analyze all these records for prominent environmental shifts and changes in the style of variability as possible influences on human evolution, dispersal, and migration. Furthermore, we examine the nonlinear dynamics with the help of recurrence plots (RPs) and recurrence quantification analysis (RQA) (Marwan et al., 2007, 2021). Here, linear correlations help to evaluate the possible existence of network edges (or hominin expansion pathways), linking eastern Africa with the northern African and Arabian hominin occupation hotspots, respectively, vertices of the network. Additionally, nonlinear recurrence analysis helps to understand what environmental opportunities or stimuli humans in the studied areas were exposed to,

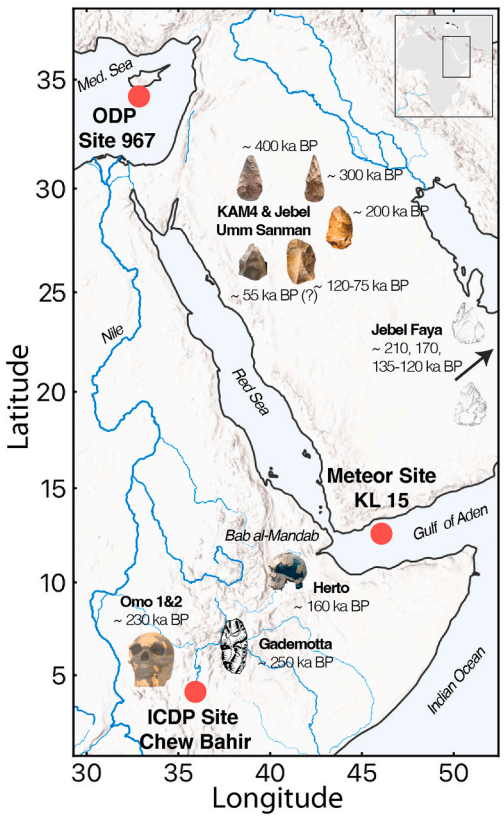

Fig. 1. Map of the study area with location of the records, important geographical and anthropological sites: ODP Site 967 (Grant et al., 2017), ICDP Site Chew Bahir (e.g., Foerster et al., 2022), Meteor Site KL 15 (this study), Omo 1 and 2 fossils (McDougall et al., 2005; Vidal et al., 2022), Herto (White et al., 2003), KAM4 and Jevel Umm Sanman (Groucutt et al., 2021), Jebel Faya (Bretzke et al., 2022), Gademotta (Sahle et al., 2014).

and either had to adapt to or escape from. Together with the recent findings of the Hominin Stes and Paleolakes Drilling Project (HSPDP, Cohen et al., 2016), during which several cores were collected from paleolakes (including the paleolake Chew Bahir) in proximity of known hominin fossil sites in the East African Rift System (EARS), the Green Arabia project (Lawler, 2014; Petraglia et al., 2015), this study provides the first high-resolution study along the African-Eurasian crossroad during the time of the emergence and dispersal of *H. sapiens*.

2. Setting and treatment of the new paleoclimate archive KL 15

The marine core KL 15 was drilled in 1987 during R/V Meteor cruise 5/2 at station 259 (12.85738°N, 47.41707°E) in the Gulf of Aden (which connects the Indian Ocean with the Red Sea) from a water depth of 1636 m (Nellen et al., 1996). The wind regime in the northwestern Indian Ocean is governed by a biannual reversal due to the monsoonal winds with SW monsoon winds from May to October and the NE winds during boreal winter. However, the Gulf of Aden's landlocked position puts it off the SW monsoon (Almogi-Labina et al., 2000). During boreal summer, Shamal winds with dust outbreaks occur. The drill site is located 80 km offshore Yemen, where no major rivers flowing into the sea.

The piston corer of 200 mm diameter initially recovered a total length of 22.12 m. The unfavorable storage conditions, which led to the core material almost completely drying out, made sampling difficult. The core was therefore first carefully moistened to soften the sediment before the samples were taken. The archive half was shrink-wrapped in film tubes, sealed, and slowly soaked with demineralized water. After three to four days, excess water was carefully removed. The uppermost sediment layer was then scraped with a spatula to remove possible

mingling during watering. After this procedure, the surface of the archive half revealed the original sedimentary structures, and, apart from shrinking, there was no evidence of disturbances compared to the original core photos. Subsequently, the sediment was transferred to U-channels for further analysis.

Age control was provided by AMS ^{14}C dating for the upper 3 m of the core and stable oxygen isotopes for the lower 19 m of the core. 21 AMS ^{14}C analyses were conducted at the Institute of Ion Beam Physics at ETH Zürich. Specimens of planktonic foraminifera species G. ruber were picked from the >300 μm fraction, carefully cracked to open chambers, and cleaned ultrasonically in highly purified water. After cleaning for 30 s, the samples were rinsed and dried in an oven at 40 °C. Radiocarbon years were calibrated to calendar years using the MARINE13 calibration curve (Reimer et al., 2013). Marine reservoir correction of $\Delta R = 187$ years was calculated from the weighted mean of the eight closest stations of published reservoir ages (Cember, 1988; Southon et al., 2002). One outlier was identified from 21 AMS ^{14}C ages, showing an age reversal, possibly due to bioturbation (see Fig. S1). The lower 19 m of the core were dated by tuning 243 samples of the δ^{18}O record of G. ruber from Almogi-Labina et al. (2000) to the LR04 benthic stack (Lisiecki and Raymo, 2005). A standard age-depth model based on 21 AMS ^{14}C ages and 243 stable oxygen isotope ages was constructed using a smooth spline regression with the R package Clam (Blaauw, 2010). Here, we used the one-sigma errors of the radiocarbon samples as provided by the AMS lab and a ±2 ka error for δ^{18}O tuning according to Lisiecki and Raymo (2005).

Loss of the original pore water led to the shrinking of the sediment. Shrinking was mainly at the top and base of the respective sections, while the middle of sections rarely show cracks. A new depth was measured from top to bottom without gaps to obtain a continuous depth scale. The resulting discrepancy of new depth positions of the lower 19 m of the core relative to their original position in the core was correlated using original full-scale core photographs acquired before shrinking. Each sample position for isotope analysis was referenced using the working half and transferred to the new composite depth. Isotope analysis samples were taken approximately every 8 cm. In total, shrinking led to a shortening of 45 cm length (corresponding to ~2% of the original length) or approximately 2 cm for each section on average. XRF scanning was conducted on U-channels with a 10 mm resolution using the Avvatech XRF Core Scanner III (Serial No. 12) at MARUM (Bremen, Germany) with a slit size of 10 mm down-core and 12 mm cross-core. A first run with 30 kV/0.6 mA and 7 s count time with a lead (thick) filter was measured for bromine, rubidium, strontium, and zirconium. A second run at 10 kV/0.04 mA and 7 s count time with no filter was measured for aluminum, silicon, sulfur, potassium, calcium, titanium, and iron. The sediment surface was covered with a 4 μm thick SPEXCerti Prep Ultralene1 foil to avoid contamination of the XRF measurement unit and desiccation of the sediment. All data were inspected, and outliers associated with cracks or uneven sediment surfaces were marked using quality flags (Fig. S2).

3. Setting and data of established paleoclimate archives

The ICDP Site Chew Bahir (CHB) composite core HSPDP-CHB14-2 was collected as part of the HSPDP during deep drilling campaigns in the EARS in 2013–2014 (Cohen et al., 2016), providing two 280 m long cores with a composite depth of ~293 m from the Chew Bahir playa lake in southern Ethiopia (4.76125°N, 36.77278°E). The ~293 m long composite core was dated using radiocarbon, ^{40}Ar/^{39}Ar, and optically stimulated luminescence combined with geochemical correlation to a known-age tephra, and the Bayesian age-depth model developed using these ages gave an age of ~620 ka (Roberts et al., 2021). The sedimentary record shows alternations of blue-green facies due to anoxic conditions and a second facies that is characterized by light brown and reddish-brown silts. The hydroclimate within the catchment is documented by the potassium (K) content of the sediment, measured by X-ray fluorescence core scanning (Foerster et al., 2012). During dry climates and associated increasing lake- and porewater alkalinity and salinity, the K concentration in the sediment increases as a result of an authigenic transformation of smectites to illites (Foerster et al., 2018; Gebregiorgis et al., 2021). Therefore, the K concentrations in the sediment are a sensitive aridity indicator mainly controlled by the paleo-hydrochemistry of the lake (Foerster et al., 2022). A new composite age model based on the Chew Bahir short core data (Foerster et al., 2012) for the uppermost part, the Bayesian age model of the HSPDP-CHB14-2 core for the middle section (Roberts et al., 2021) and a tuned age model for the lowermost section of the same long core, the ~293 m composite core shows an average sedimentation rate of 0.5 m per ka (Trauth et al., in review).

The marine core at ODP Site 967 at 34.068°N and 32.725°E, located in the eastern Mediterranean, northern Eratosthenes Seamount, at a water depth of 2252 m, was obtained during ODP Leg 160 (Emeis et al., 1996). The record has a length of approximately 90 m with sediments from the Pliocene to the Holocene. The sediment consists of hemipelagic bioturbated nannofossil oozes and nannofossil clays, including 79 sapropels and several thin turbid layers (Larrasoaña et al., 2003). We used the wetness index from Grant et al. (2017) as a record of wetness in the source regions of Saharan and northern African dust and, beyond this, as a record of the influx of the river Nile since the wetness index is a measure that combines both runoff and dust signals. This wetness index is based on a newly calibrated XRF dataset and its combined first and second principal components representing detrital input and a sapropel signal. This allows observing the effects of both the expansion and intensification of the northern and northeastern African monsoon (manifested as increased runoff) and its retreat and weakening (manifested as increased dust) (Grant et al., 2017).

4. Data analysis methods

The XRF data set of the KL 15 core includes 2167 data points with a resolution of one mm, corresponding to 546,000 years. We carefully preprocessed the data before we tested for correlation with the neighboring data sets from eastern Africa and the eastern Mediterranean using linear and nonlinear methods. One of the preparations (and preliminary considerations) concerns possible dilution effects (so-called closed sum effects) typical for compositional data. This effect describes that each possible combination of all existing n elements of the XRF dataset (e.g., potassium, iron, titanium, calcium, and others) forms the simplex of the n-dimensional data space. Each measure is located on that simplex, leading to dependent measurements due to the dilution effect.

Such dilution effects are certainly to be expected in the marine core KL 15, as the high content of calcium in particular leads to an apparent negative correlation between carbonate and all other elements. One technique to overcome the problems due to the nature of compositional data is the log-ratio transformation (Aitchison, 1982). The logarithm of a simple (and symmetric) ratio between two components (element counts) is a straightforward type of transformation. Here, the transformed data inherits the dynamics of the two elements forming the ratios but discards the dissolution effects of the other n-2 components. This reduced data set allows the analysis of temporal system-inherent patterns if well-correlated projections of the underlying climate process on the proxies have been identified.

In contrast to core KL 15, such dilution effects are not to be expected with the composite core from ICDP Site Chew Bahir, as no element (especially not calcium) reaches concentrations such that it could dilute other elements. Nevertheless, log-ratios were used in some studies (e.g., log(K/Zr) in Schaebitz et al., 2021), even if this was not absolutely necessary, and in the case of the more stochastic Zr concentrations it may even have an unfavorable effect on the signal-to-noise ratio of the signal. For this reason, log-ratios were avoided in studies in which the application of sophisticated statistical methods were in focus (e.g., in Trauth et al., 2021b), as it is the case in the present study.

To understand what processes lead to the chemical composition of the sediment mapped in the XRF dataset and to find a suitable proxy of the Arabian Peninsulas hydroclimate, we used a pairwise Euclidian distance matrix, created a hierarchical cluster tree, and presented it in a dendrogram (Fig. 2). Low values between pairs of observations (elemental counts) of this symmetrical matrix indicate a low distance within the n-dimensional data space and, hence, a proposed processual link. The hierarchical cluster tree is calculated using the Ward method (Ward, 1963) and agglomerates the distances hierarchically. Based on this dataset exploration, we compared log(Ca/Ti) and log(Ti/Al) with the grain size data from core KL 15 from Fleitmann (1997) to identify a proxy for the Arabian Peninsula's hydroclimate. We then correlate this proxy record with those from the other two sites, ODP Site 967 and ICDP Site Chew Bahir, to decipher regional from supra-regional and global signals, facilitating an understanding of the spatio-temporal variation of environmental change and its causes. The Spearman rank correlation coefficient (Spearman, 1904) is a simple non-parametric method to estimate the correlation between pairs of observations, e.g., time series. We use the Spearman coefficient with a window size of 50 ka (to avoid aliasing effects) to analyze the pairwise cross-correlation between the three records representing the eastern African, Nile-Mediterranean, and Arabian hydroclimate.

Besides the correlation of the climate proxies using correlation techniques, the temporal dynamic of the system with its state variables (i.e., the interacting components such as wind, precipitation, temperature, vegetation, and others) is of interest, as it may capture the system's inherent mechanisms (Trauth et al., 2021b). The phase space of the system's state variables can be reconstructed using the proxy-based one-dimensional projection of the original phase space. This reconstruction is done by time delay embedding (Packard et al., 1980), which unfolds the phase space portrait, as explained in detail by Marwan et al. (2007) and Trauth et al. (2019, 2021). By principle, a single proxy (such as log(Ti/Al) or K counts) that represents a mixed signal of the hydroclimate is used to reconstruct continuously the relative proportions (the so-called phase space) in between the original state variables (e.g., wind, precipitation, temperature, vegetation). Analyzing the phase space

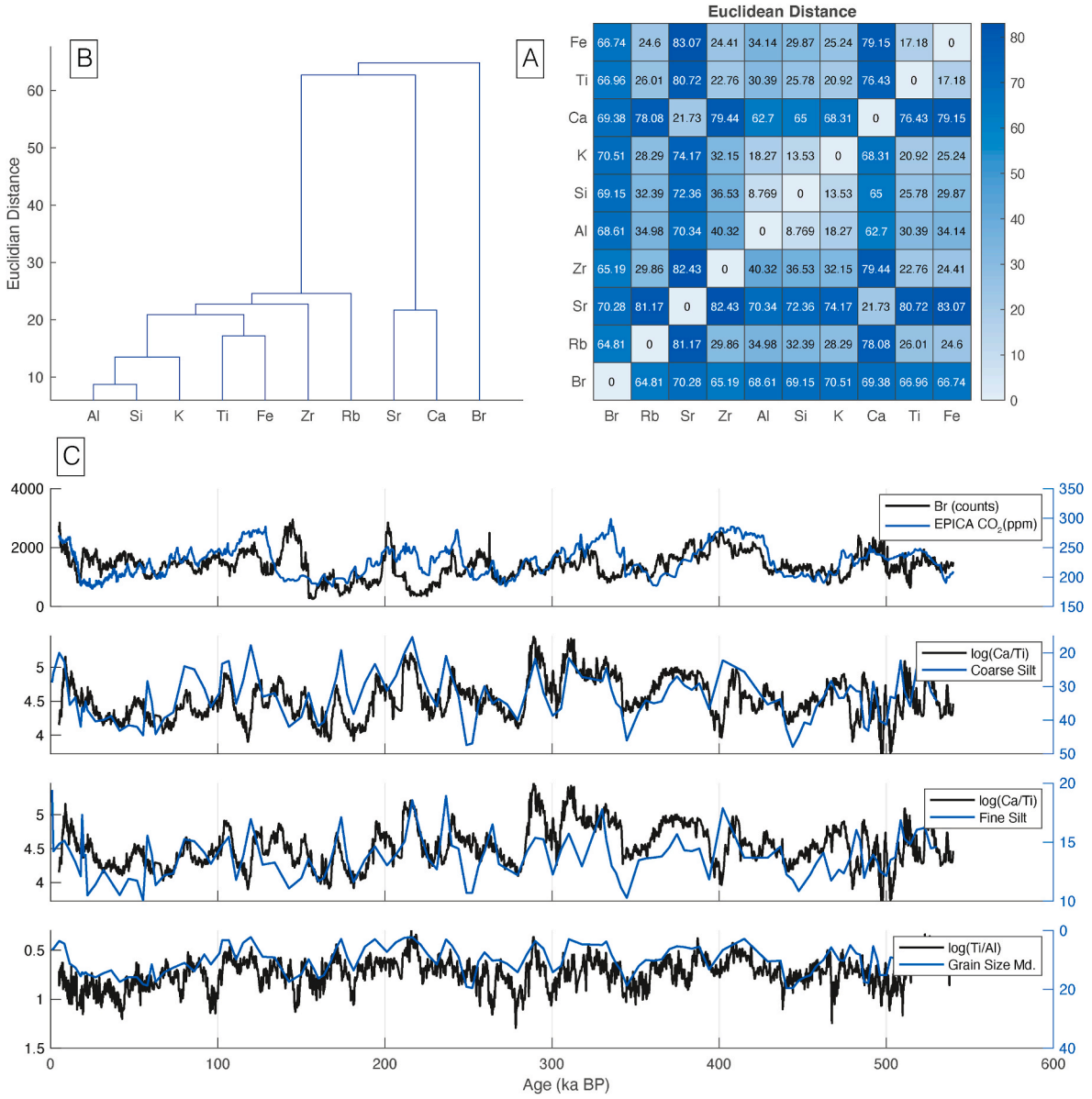

Fig. 2. Analysis of the XRF dataset of the marine core from Meteor Site KL 15 with (A) pairwise Euclidean distance between the element counts; (B) dendrogram of the Euclidean distance between the XRF counts of the KL 15 marine core; (C) Br counts and LR04, log(Ti/Ca) and inverted coarse silt, log(Ti/Ca) and fine silt, and log (Ti/Al) and median grain size. Grain size data from Fleitmann (1997).

portrait is done by visual inspection of the resulting recurrence plot (RP) together with a recurrence quantification analysis (RQA), foremost using the measures recurrence rate (RR) and determinism (DET) (Marwan et al., 2007; Trauth et al., 2019). Hereby, an RP is a binary matrix based on the thresholded comparison of the (for example) Euclidian distance between the reconstructed phase space states.

A visual inspection of occurring patterns may allow inferences regarding the system's inherent mechanisms, e.g., cyclic, static, or stochastic, and regarding significant transitions and other discontinuities within those climate dynamics (Trauth et al., 2019). RR and DET are calculated using windowed sections of the RP. Herein, RR, as the proportion of recurring states in relation to all states within a given window, describes the probability of recurring states (Trauth et al., 2021b). DET is the proportion of recurring states forming diagonal lines out of all recurring states, describing (but without actually claiming) the predictability of the system, as diagonal lines in an RP mark episodes with cyclic (but not necessarily sinusoidal) behavior. RR and DET provide complementary information about the underlying system dynamics, with high values characterizing a recurrent and deterministic system. In contrast, low values indicate a more stochastic system, meaning no or less recurring of states and non-predictable dynamics. We first chose the most suitable embedding parameters to calculate the RP, as explained in Marwan et al. (2021) and Trauth et al. (2019, 2021). Here, we use the parameters $m = 5$ and $\tau = 10$, which equals a time of 1 ka at a given temporal resolution of 100 years. We then calculate the RP and their respective RR and DET of the three records for a sliding window of 50 ka (again to avoid aliasing effects with the precession). Finally, we compare major climate phases (based on the linear and non-linear time series analysis) with milestones in human evolution, migration, and innovations to draw conclusions and to postulate ideas about the spatio-temporal shifts in climate between our three sites and how they could have influenced human livelihood.

5. Data analysis results

In this study, we have examined the cores of three sites. The (Meteor Site KL 15 is examined by us, the records of the ICDP Site Chew Bahir have been extensively published, but we have re-examined the published data for this study. We also re-examined the published records of the ODP Site 967 (Grant et al., 2017).

The marine core from Meteor Site KL 15 covers the past 546 ka with an average sedimentation rate of ~4 cm/ka based on our updated age model. The dendrogram of the pairwise Euclidian distances of the XRF dataset reveals three major groups (Fig. 2): The first group includes the subgroup of aluminum and silicon, potassium, iron and titanium, zirconium, and rubidium. The second group is strontium and calcium, and the third group, with the highest Euclidian distance to the rest of the dataset, includes only bromine. Bromine shows a weak correlation with atmospheric CO_2 from EPICA (Bereiter et al., 2015). The log-ratio of calcium and titanium is negatively correlated with the coarse silt and positively correlated with the fine silt. The log-ratio of titanium and aluminum shows the same tendency as the median grain size but with higher variability.

Sediment composition at Meteor Site KL 15 is predominantly controlled by carbonate, as suggested by the high carbonate contents of ca. 56% on average and their variability of 45 to 65% (Stein et al., 2007). Furthermore, heavy minerals and organic matter contribute significantly to the composition, grain size distribution, and overall character of the sediment. These three groups (carbonates, heavy minerals and organic materials) are clearly visible in the dendrogram of the Euclidian distance. Bromine, representing the third and smallest group, is interpreted as a productivity proxy (e.g., Ziegler et al., 2008). The correlation with the EPICA atmospheric CO_2 in sections emphasizes the sensitivity of the marine environment of the Gulf of Aden to variations in greenhouse gas concentrations. The loss of this correlation in some sections may indicate another factor, for instance, the effect of the northeastern winter monsoon (Almogi-Labina et al., 2000).

Using the correlations of titanium and calcium with grain size, however, either as raw counts or in log-ratios with other elements to correct Ti counts for the dilution by Ca in terms of an Aitchison log-ratio transformation, it becomes clear that Ca is mainly present in the fine silt fraction, while titanium is mainly found in coarse silt. Presumably, foraminifera shells are by far the most important carrier of the Ca signal, although lateral displacement of the shells by deep water currents and the associated grain size sorting can distort the primary signal (McCave and Hall, 2006; Mesa-Fernández et al., 2022). Since Ti is primarily found in coarse silt, typically the grain size of wind-blown terrigenous detritus, we hypothesize dust transport is the dominant process behind the Ti signal (Fleitmann, 1997; Nicholson et al., 2020). We hence use Ti, in a log-ratio with aluminum (Al) to correct for dilution effects due to Ca, as a proxy for aeolian input and, hence, as an aridity index, which is further supported by the fact that both are part of the major subgroups of the terrigenous input within the Euclidian distance dendrogram (Fig. 2), whereby aluminum is allocated close to silicon and titanium close to iron (e.g., Calvert and Pedersen, 2007; Jimenez-Espejo et al., 2008; Konijnendijk et al., 2014, Ehrmann et al., 2024).

Testing for correlation of the KL 15 aridity index with the Chew Bahir aridity index, we find positive correlations between 400 and 150 ka BP (Fig. 3). After ~150 ka, we find a negative correlation. Still, a significant gap due to core loss in the Chew Bahir record reduces the statement's reliability for the middle part of this interval. Correlating the KL 15 record with the ODP Site 967 record is hampered by the low sedimentation rate of 2–4 cm/ka in the eastern Mediterranean Sea (Grant et al., 2017). The wetness index from ODP Site 967 shows much less submillennial variability than the records of KL 15 or Chew Bahir, possibly due to climate signals modulated by a combined effect of a larger distance to a huge catchment area with low relief and different climatic influences, some of which cancel each other out. Correlations with the other records occur in episodes, both positive to KL 15 and Chew Bahir between ~400 and 150 ka, and either positive or negative correlations occur before and after this time interval.

The analysis of RPs, showing both similarities and differences between the three sites, helps us to understand the climate dynamics in northeastern Africa and Arabia (Fig. 4). Particularly striking is a major shift in the RPs of all three records at ~400 ka, whereby the character of this transition differs greatly from all other shifts in the RP due to the occurrence of different, mostly blocky structures before and after it. Secondly, the fragmented nature of the RPs of ODP Site 967 and Chew Bahir is obvious, in contrast to the RP of KL 15. In the RPs of ODP Site 967 and Chew Bahir, major transitions separate two distinct blocky structures not present in the RP of KL 15. Third, the RPs of Chew Bahir and ODP Site 967 show distinct shifts at ~130 ka, whereas the RP of KL 15 shows a similar transition at ~70 ka. For the time period between ~150 and 50 ka, the RPs contain similar features, with a blocky structure in the RP of ODP Site 967, a two-part blocky structure with millennial-scale cyclicities in the RP of Chew Bahir, and a relatively unstructured first half and a blocky second half of the RP of KL 15.

RQA helps with a deeper understanding of the structures of the RPs, in our example, by using the RQA measures DET and RR. Before ~400 ka, ODP Site 967 shows a higher DET than in the epochs later and recurring diagonal lines at intervals of a few millennia, indicating an oscillating, and thus predictable, climate on this time scale. In contrast, the RP of Chew Bahir indicates relatively stable phases, separated by abrupt shifts on precession time scales. KL 15 has short periods of oscillating climate before ~400 ka BP with a similar precession cyclicity. Here, the ~400 ka BP transition is less pronounced, marked by a change in the frequency of recurring events and a generally high DET. In contrast, the RP of Chew Bahir shows a shift with a decrease in DET that is followed by a period from ~400 to 350 ka BP with a higher RR. At ODP Site 967, the highly deterministic time ends at the ~400 ka BP transition, followed by ~150 ka BP with a low DET. Chew Bahir has periods of increased RR from ~400 to ~350 ka BP and, then again, at

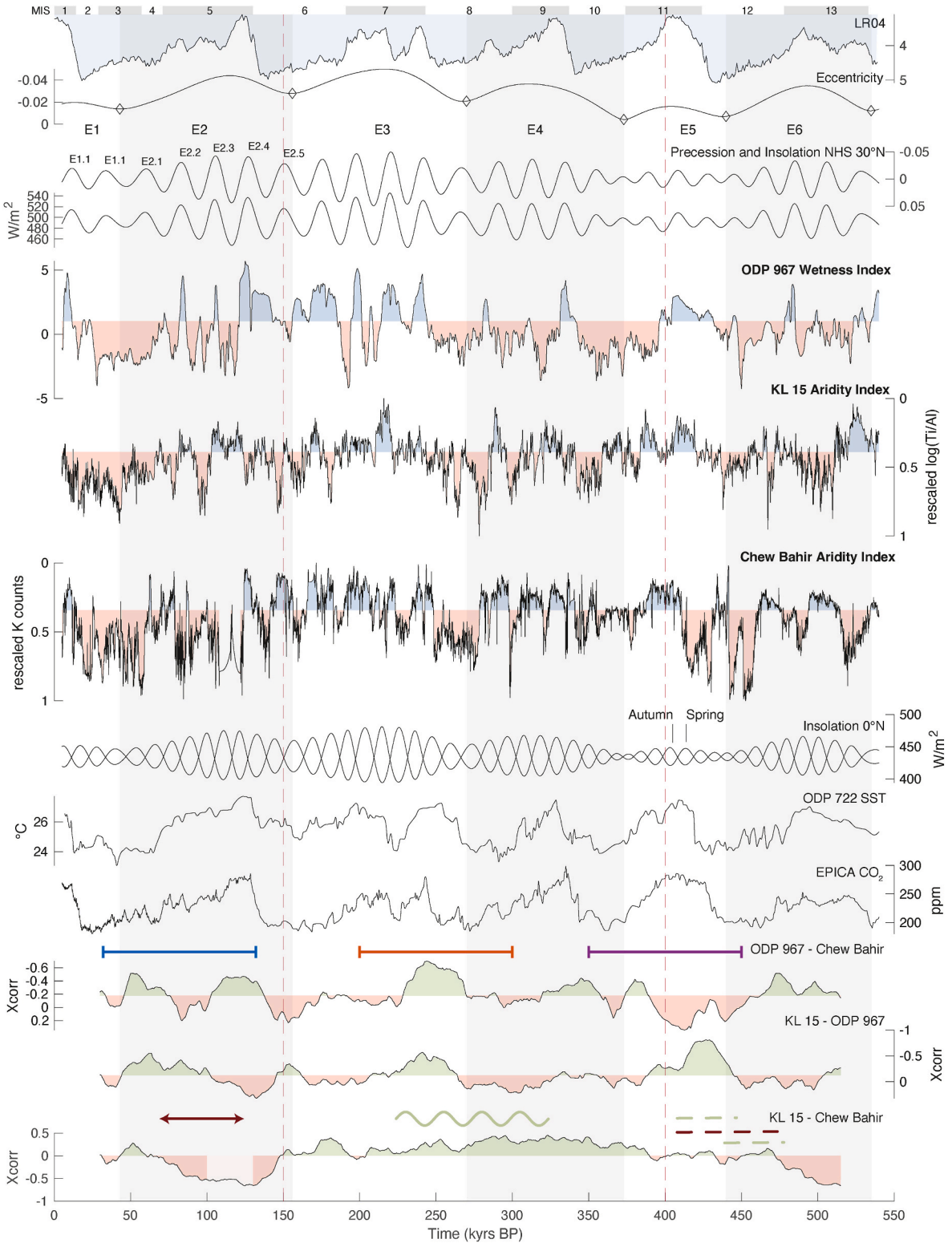

Fig. 3. Time series of the analyzed records with (from top to bottom) marine isotope stages (Railsback et al., 2015), LR04 benthic stack (Lisiecki and Raymo, 2005), eccentricity with labeled minima and respective shaded background (Laskar et al., 2004), precession and boreal summer insolation at 30°N (Laskar et al., 2004), ODP Site 967 wetness index (Grant et al., 2017), Meteor Site KL 15 aridity index based on log(Ti/Al) (this study), ICDP Site Chew Bahir aridity index based on K counts (this study), equatorial spring and autumn insolation (Laskar et al., 2004), ODP Site 722 sea surface temperature reconstructions (Herbert et al., 2010), Epica $CO_{2,atm}$ concentrations (Bereiter et al., 2015), and cross-correlations with a 50 ka window between records from ODP Site 967 and ICDP Site Chew Bahir, Meteor Site KL 15 and ODP Site 967, and Meteor Site KL 15 and ICDP Site Chew Bahir (this study). Blue, orange, and purple bars mark time sections of relevant changes in the determinism (Fig. 04). Red arrow, green curve, and red/green dashed line mark major time sections of relevant correlations between the records from Meteor Site KL 15 and ICDP Site Chew Bahir. (For interpretation of the references to color in this figure legend, the reader is referred to the Web version of this article.)

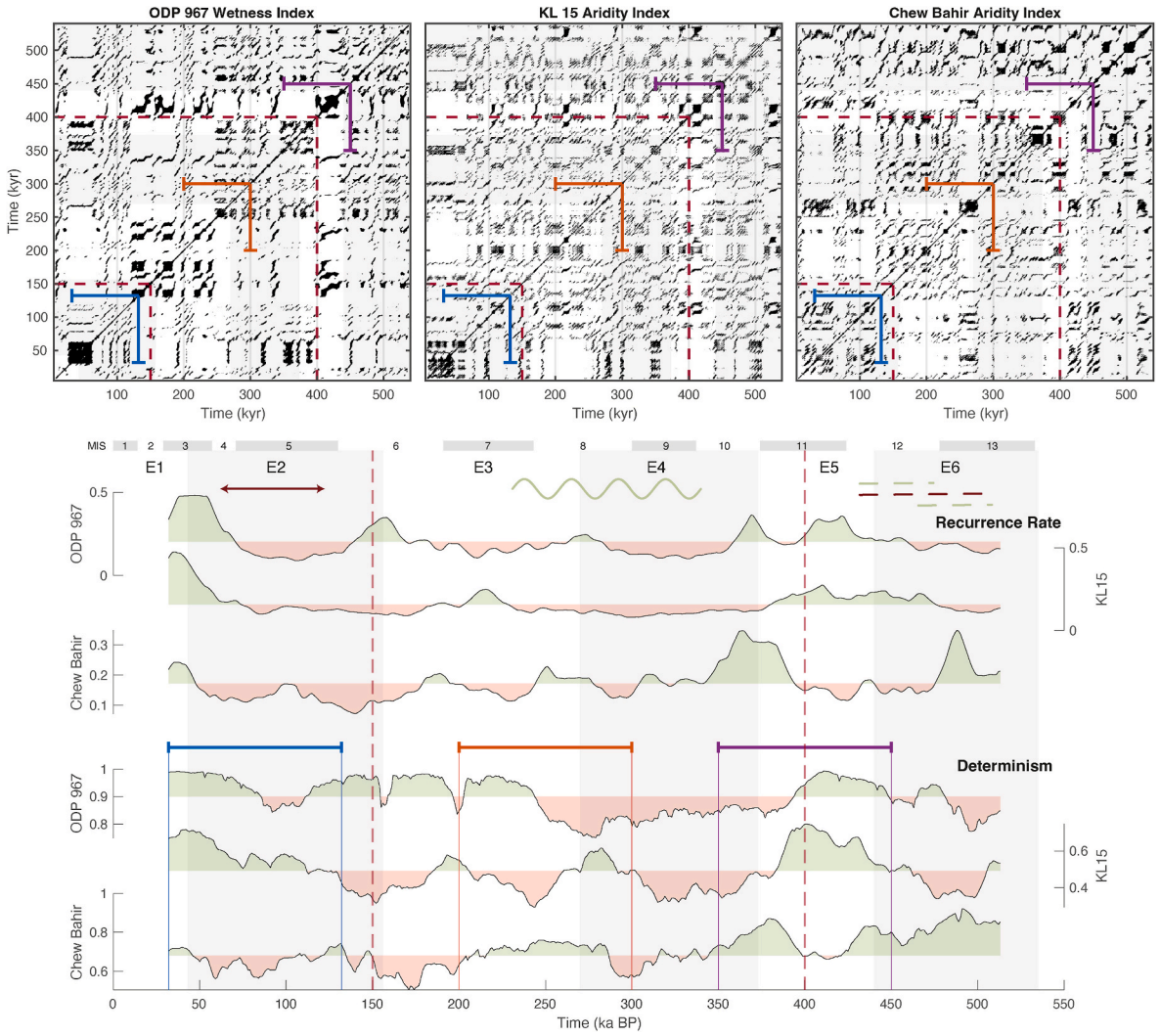

Fig. 4. Recurrence plots and recurrence quantification analysis with the recurrence rate and determinism of the three analyzed records with major time section breaks based on ICDP Site Chew Bahir and Meteor Site KL 15 cross-correlation analysis (dashed line) and important time sections (colored bars). All three time series are interpolated to an evenly spaced time series with a resolution of 0.1 ka from 5 to 540 ka. Embedding is proceeded with $m = 5$; $\tau = 10$. The threshold for recurrence is calculated under a variable threshold with a fixed amount of nearest neighbors in the phase space. The window size for calculating the recurrence rate and the determinism is 500 data points or 50 ka.

~250 and ~180 ka BP.

The climate shifts between recurring diagonal lines with millennial spacing (e.g., KL 15) and more prominent blocks with distinct shifts in the RP of Chew Bahir. Following the ~250 ka BP transition, as visible in the RPs, all three sites show increasing recurrences, as indicated by the occurrence of distinct diagonal lines in their respective RPs. Hereby, KL 15 has the highest frequency (lowest distance between the diagonal lines) and shows multiple separated blocks with similar internal structures. Chew Bahir has a long-lasting time of consistent recurring patterns that ends at around ~130 ka BP. The DET of ODP Site 967 increases after ~250 ka BP and is then disrupted at ~200, ~160, and ~100 ka BP. Chew Bahir has high DET (compared to the time before and after) from ~300 to ~200 ka BP and then again, for a short period of time, at around 120 ka BP. The low DET in the RP of Chew Bahir between ~100 and ~50 ka BP is accompanied by increased DET in the RP of KL 15 and, with time delay, in the RP of ODP 967.

6. Discussion

Using the newly established hydroclimate proxy from Meteor core KL 15, we correlated three key archives to reconstruct environmental changes during the past ~550 ka. The three sites are lined up in pairs along two possible expansion trajectories of H. sapiens (e.g., Armitage et al., 2011). When comparing the environmental conditions along this S-N axis (ICDP Site Chew Bahir, ODP Site 967) and NE-SW axis (ICDP Site Chew Bahir, Meteor Site KL 15), our null hypothesis is that changes have the same sign and a similar magnitude, which would be expressed in a positive correlation and similar dynamics in the RQA measures of the respective RPs (Figs. 3 and 4). Such synchronization is plausible because of the regional climate's response to orbitally controlled solar radiation, which is latitude-dependent. Differences in the magnitude and sign may occur, especially along the ~3300 km long N-S axis between ICDP Site Chew Bahir and ODP Site 967. It has been shown that the local solar radiation is of greater influence at times of maximum eccentricity. In contrast, at times of low eccentricity, the boreal summer insolation dominates (e.g., Trauth et al., 2003; Clement et al., 2004; Kutzbach et al., 2020). This happened most recently during the ~10 ka BP boreal summer insolation maximum in the current phase of low eccentricity, when hydroclimate had changed in northern Africa in phase on orbital (but not shorter) time Scales (Kutzbach and Street-Perrott, 1985; Pausata et al., 2020). Together with strong positive vegetation feedback, this constellation led to the last Green Sahara Phase, when

today's arid to hyper-arid Sahara was widely populated by humans living along extensive systems of rivers and lakes (e.g., Kuper and Kröpelin, 2006; Drake et al., 2011).

The direct correlation between hydroclimate proxies from different sedimentary records inherits uncertainties and potential failures due to the nature of paleoenvironmental research. Among a wide range of factors such as site-specific proxy processes and different scaling, this includes (1) limited sample sizes of usually only a few cm^2, and (2) age models that are based either on direct ages or tuned proxies. While the first problem can be potentially countered by an increase in sample sizes (limited by funding or the number of parallel investigated destructive proxies), the latter can be tested using different solutions of the age-depth relation. Here, we compare three archives: two from a marine environment with tuned age models and one from a terrestrial fluvio-lacustrine archive with a directly dated Bayesian age model. The terrestrial archive, ICDP site Chew Bahir, has a two-sigma range of ca. 40 ka, especially for the section between 75 and 234 m core depth. Therefore, parallel to this study, we developed a new tuned age model (Trauth et al., in review) to acknowledge the variety of sedimentation rates due to the nature of a fluctuating lake environment at the Chew Bahir basin and used this tuned age model for comparison. As shown in Fig. S5, the complementary solution for the correlation experiment does show the same overall correlation pattern. Still, the precession-scaled hydroclimate variability is in parts off-phase to the record from the KL 15 site.

Examining the pairwise correlation of the three sites, a predominantly positive correlation between ICDP Site Chew Bahir and Meteor Site KL 15 is noticeable in the period **between ~400 and ~150 ka BP** (Fig. 3). These correlations are most prominent in times of high eccentricity – and thus a dominance of regional-seasonal vs. Boreal summer insolation. As the two sites are only 8 degrees of latitude apart from each other, this is not surprising. The resulting temporal difference between the local insolation maxima at times of solar zenith is thus only ca. 2 ka and thus shorter than the time scales considered here. The relationship between these sites and ODP Site 967 is more complex. Although, within the uncertainties of the respective age models, there are indeed similarities in the long-scale variations, but the obviously much more muted response of the site to influences shorter than eccentricity leads to an alternation of positive and negative correlations with the other sites. As the southern sites are largely synchronized between ~400 and ~150 ka BP, the correlation of ODP Site 967 with these sites shows some similarities, as expected.

There are alternative explanations for the evolution of the wetness index of ODP Site 967. It should be noted that this index integrates over several latitudes from the equator across the eastern Sahara to the Nile delta: it is a moisture index of northern Africa, quite different from the other two sites with comparatively smaller climate signal integration. This could be the reason for the smooth curve, which is expressed in a strong time-scale dependent correlation with the detailed curves from the southern sites. However, looking beyond the orbital forcing, we find a good match between ODP Site 967's wetness index and the atmospheric CO_2 concentration ($CO_{2,atm}$): it is wet in northern Africa when $CO_{2,atm}$ is high. This is what we expect since $CO_{2,atm}$ is one of the main factors influencing vegetation (and therefore also, along with humidity, a green Sahara). The strong vegetation feedback amplifies the effect, so the increase in vegetation cover shifts the climate towards even wetter conditions (Otto-Bliesner et al., 2014; Kutzbach et al., 2020). Supposing this interpretation of the different sites and the corresponding proxies is correct, the ICDP Site Chew Bahir and Meteor Site KL 15 reflect the conditions at possible destination areas and major network vertices of hominin expansion and occupation. ODP Site 967, on the other hand, integrates the conditions on the way north and the possible destination area of expansion there.

The good agreement between the southern sites between ~400 and ~150 ka BP is absent in the period **earlier than ~400 ka** BP when there is no simple pattern, with partly opposing trends in humidity. Positive correlations occur, but often only for a short time of a few millennia, and are doubtful due to the increasing uncertainty in the age models as core depth increases. A possible reason could be the low eccentricity and, thus, the low amplitude of the precession, which reduces the role of the local orbitally driven insolation on the water cycle (Trauth et al., 2003). Instead, in ODP Site 967, as thereafter, an influence of $CO_{2,atm}$ may play some role, while there are interesting correlations of the southern sites with Indian Ocean surface water temperatures. Some of the rapid dry-to-wet transitions there, e.g., at ~420 ka BP, could be due to a rapid increase in sea-surface temperatures (SSTs, Herbert et al., 2010), although this correlation may well be a coincidence, and this interpretation is more speculative. However, should these differences between sites be real, they are certainly important factors affecting the expansion of humans, for example, when there are opposing trends such as between Chew Bahir (towards drier conditions) and KL 15 (wetter conditions) before ~470 ka BP, as clearly indicated by the pronounced negative correlation in our results.

The importance of the **~400 ka BP transition** is supported by the nonlinear analysis of the climate system, as it is clearly visible in the RPs (Fig. 4). The regime in the more northern-located sites (ODP Site 967 and Meteor Site KL 15) shifts from a deterministic behavior to more erratic blocks, which represents a less deterministic and less recurrent climate dynamic. In contrast, ICDP Site Chew Bahir changes from a less deterministic (~430 to ~400 ka BP) to a more deterministic, highly recurrent, and, in this case (but not necessarily), also more stable (~400 to ~350 ka BP) hydroclimate pattern. Though speculative, the decrease in amplitude of the precession weakens the primary controlling factor close to the equator where insolation is greatest, whereas $CO_{2,atm}$ or SSTs govern the hydroclimate in the more northern areas. After the ~400 ka BP transition, $CO_{2,atm}$ and Indian Ocean SST decrease, reducing the controlling factors of the northern sites and de-forcing equatorial hydroclimate (ICDP Site Chew Bahir) to a more deterministic state. Then, from ~280 to ~200 ka BP ICDP Site Chew Bahir shows more deterministic climate dynamics, contrary to the Arabian hydroclimate signal from Meteor Site KL 15. Here, Chew Bahir's hydroclimate might be controlled again by the precessional heartbeat of the tropics, leading to a variable but deterministic (more predictable) hydroclimate until eccentricity reaches a maximum at around 200 ka BP.

The time **after ~150 ka BP** also shows an inconsistent picture, which has other influencing factors than orbitally-controlled insolation variations, again possibly due to the reduced eccentricity. In the first half of this period, approximately between 150 and 75 ka BP, a clear precession cyclicity can be seen, but in opposite directions between the southern sites, which is expressed in a negative correlation. After ~75 ka BP, this pattern gets less clear. The precession-driven oscillation of the climate weakens, while all three sites show a clear trend towards arid climates, starting slightly earlier in the north than in the south, before all three sites show a clear African Humid Period/Green Sahara. This trend is accompanied by a decrease in climate determinism in the more equatorial ICDP Site Chew Bahir, whereas Meteor Site KL 15 shows an increase in DET. The differences between 150 and 75 ka BP, a time when the influence of the eccentricity is still visible, are due to differences in the influence of local insolation (e.g., Trauth et al., 2003). While the precipitation seasonality is bimodal (Mai-April and November-December rains) close to the equator, the Sahara–Nile rainfall is unimodal (boreal summer rain) (Palmer et al., 2023). The modern-day partly hyper-arid Arabian Peninsula received unimodal precipitation due to a northward shift of the African rain belt during times of low precession and, hence, increased northern hemisphere summer insolation (Kutzbach et al., 2020). In contrast, tropical rainfall may be enhanced during precessional-caused increased insolation during spring and autumn, doubling the frequency with a phase lag to the increased boreal summer insolation cycle (Trauth et al., 2003; Verschuren et al., 2009). So then, if the precessional amplitude surpasses a threshold, the orbital pacemaking weakens, causing asynchronously enhanced precipitation.

The correlation of climatic conditions at the three vertices of the triangular network reveals important links between eastern Mediterranean, eastern Africa, and Arabia, facilitating hominin migratory movement at times, and/or hampering it at other times. The three areas show intermittent synchronized climate dynamics on orbital time scales, at the same time when synchronization does not necessarily exist on shorter (millennia, centuries) time scales (Fig. 5). However, a link between major vertices that facilitates migratory movement due to favorable conditions (e.g., Beyer et al., 2021) is more likely to be established during times of synchronized climate dynamics, even if it may only last for a few centuries to millennia. The pattern of spatiotemporal synchronization between the three vertices of the triangular network fundamentally changed after 150 ka BP when the synchronized climate dynamics between eastern Africa and Arabia that had lasted from 550 to 150 ka BP ended. Then, a variable network link availability between the eastern Mediterranean, eastern African, and Arabian areas was established. This is indeed fascinating because this change from relatively stable conditions to great variability coincides with the second out-of-Africa migration via the northern Nile-Levantine route, when an increased availability of links between eastern Africa and the eastern Mediterranean from 130 to 100 ka BP is observable (Fig. 5). Furthermore, our data corroborate an increased availability of spatial links in the Levantine-Arabian subregions from 100 to 40 ka BP when stone tools indicate occupation in Arabia (Groucutt et al., 2018, 2021, Fig. 1), and, presumably, an unsuspected extended period of genetic adaptation of *H. sapiens* occurred (Tobler et al., 2023).

The validation of the proposed model, which explains changes in human behavior through spatiotemporal changes in climate dynamics at spatially connected regions, is difficult because fossil- and artifact finds are naturally incomplete, often inaccurately dated, and hence tentative (Bergström et al., 2021; Faith et al., 2021). Both fossil- and tool finds often show a bias due to a preservation artifact, i.e., finds are more likely to be preserved in fluviolacustrine sediments, formed during rather humid climates (Maslin and Trauth, 2009; Hopley and Maxwell, 2022; Faith et al., 2021). This widely leads to attempts to explain human behavior governed by climate change alone and, particularly in this context, with wet-dry transitions. For instance, the occupation at the mountainous site Jebel Faya seems to have been by far more continuous than earlier anticipated and not necessarily tied to wet-dry changes (Bretzke and Herkert, 2023). The simple one-to-one causality of climate change and human behavior is also countered by the well-known adaptive capacity of humans: behavioral flexibility may allow adaption to multiple climate states, dynamics, and ecological niches (Potts, 1998; Grove, 2014; Maslin et al., 2014, 2015). This is aggravated by the fact that mountainous regions offer a much wider range of niches due to the orographic stratification of biomes, whereas lowland biomes are

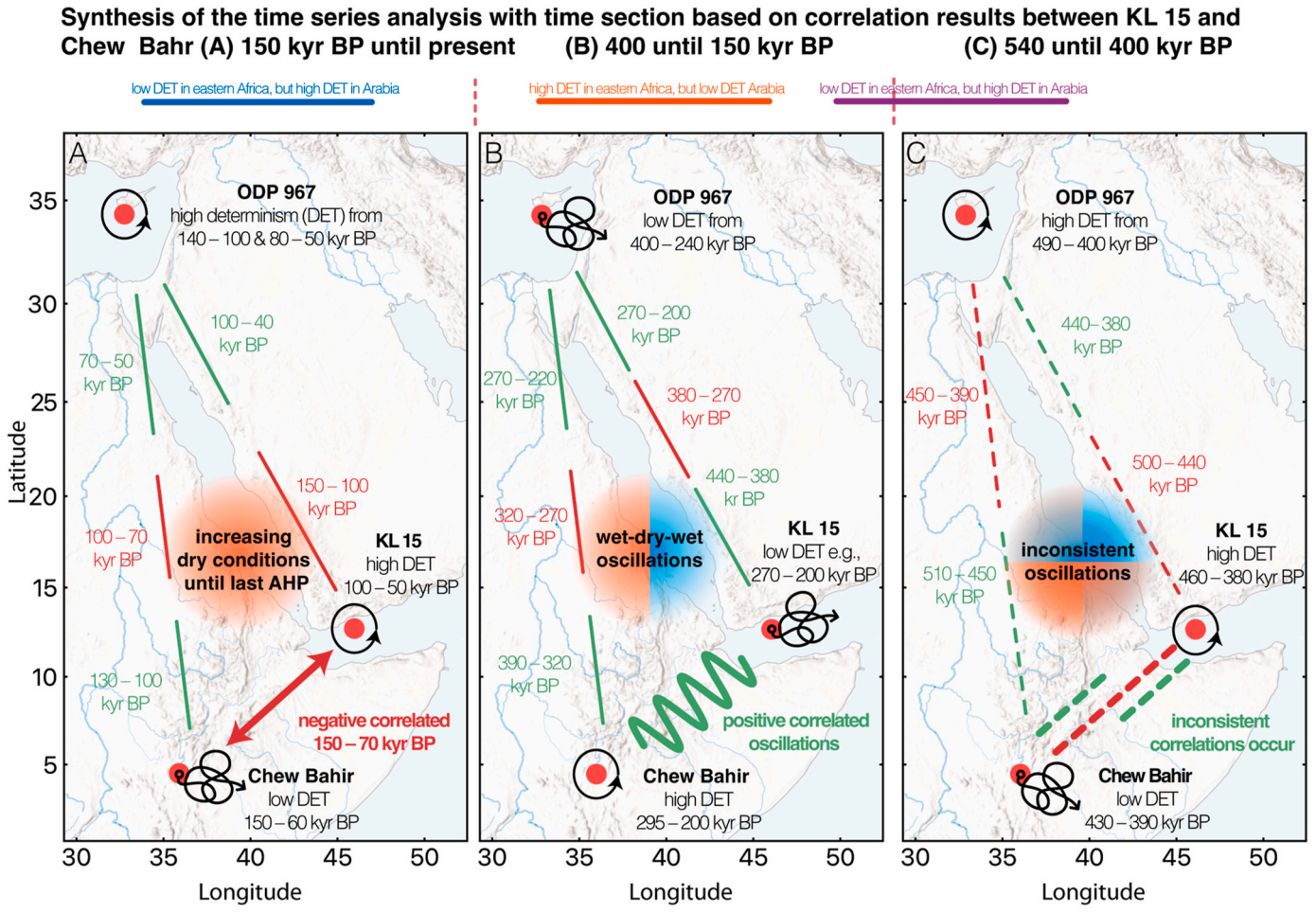

Fig. 5. Synthesis maps of the analyzed time series with three key phases of paleoclimate dynamics between eastern Africa (ICDP Site Chew Bahir record) with Arabia (Meteor Site KL 15 record) with (A) time section from 150 ka until present indicated by thick red double arrow, (B) 400 to 150 ka with positive correlations between ICDP Site Chew Bahir and Meteor Site KL 15 on a precessional time scale indicated by a green sinusoidal curve and (C) 540 to 400 ka with unclear correlation signals between ICDP Site Chew Bahir and Meteor Site KL 15 indicated by dashed lines in green and red. Blue, orange, and purple bars for temporal orientation indicate time sections of diverging DET dynamics. The black circled arrow indicates a specific time of high DET in the record. The undirected arrow indicates phases of low DET. Red lines indicate phases of negative correlation between two records, whereas a green line indicates a time when positive correlations occur. (For interpretation of the references to color in this figure legend, the reader is referred to the Web version of this article.)

clearly disadvantaged in the availability of water and food (King and Bailey, 2006). It is, therefore, conceivable that climate shifts in lowland regions only allow for behavioral flexibility and continuous occupation in times when climate changed rather gradually, following recurring (cyclic or more complex repetitive) patterns and, therefore, was more predictable. If the climate is characterized by recurring patterns on a centennial time scale, behavioral strategies could have been developed, allowing *H. sapiens* to adapt to changes, either through experience (or memory) of similar patterns from the past, or through ideas for new strategies for survival.

In our study, we see a clear correlation between a predictable climate and accompanying environmental living conditions, within the aforementioned uncertainties, recognizable by higher DET values in the RPs of the corresponding paleoclimate time series (Figs. 1 and 5). Higher DET values do not necessarily mean that the climate was particularly stable or particularly humid. Predictability can certainly mean variability. For example, at KAM4 and Jebel Umm Sandman in Arabia, major occupation phases, such as during 200, 120-75, and 55 ka BP (Groucutt et al., 2021) coincide with times of increased DET in Arabia. The Omo 1&2 fossils (McDougall, et al., 2005; Vidal et al., 2022), the Herto fossils (White, et al., 2003), and the Gademotta stone tools (Sahle et al., 2014) in eastern Africa cohere with phases of increased DET but not with times of a stable or wet climate (Figs. 1 and 5). Also, the proposed 30 ka adaption time, presumably in Arabia, would cohere with a time of increased DET in Arabia (Tobler et al., 2023). Though still speculative, a predictable climate, even if it is variable, described by an increase in the DET in the RPs, would provide opportunities or even stimuli, favoring or vice versa disfavoring occupation, migration, and expansion throughout the different occupied hominin network vertices, such as eastern Africa and Arabia.

7. Conclusion

Analyzing the new aridity index from Meteor Site KL 15 together with the established aridity index from ICDP Site Chew Bahir and the well-known wet-dry index from ODP Site 967 using linear correlation and nonlinear recurrent analysis for the past 540 ka revealed three major phases of spatiotemporal dynamics within this triangular network. We observe major shifts in the climate dynamics at 150 and 400 ka, presumably governed by changes in the amplitude of the orbital eccentricity. We see positively correlated network links concordant to supposed major migration phases of *H. Sapiens*. Furthermore, we do see rather an accordance of human settlement rather during times of a predictable climate than during specific of humid climates.

CRediT authorship contribution statement

Markus L. Fischer: Conceptualization, Data curation, Formal analysis, Visualization, Writing – original draft, Writing – review & editing, Investigation, Validation. **Philipp M. Munz:** Conceptualization, Data curation, Formal analysis, Investigation, Resources, Writing – review & editing. **Asfawossen Asrat:** Conceptualization, Writing – review & editing. **Verena Foerster:** Conceptualization, Investigation, Writing – review & editing. **Stefanie Kaboth-Bahr:** Conceptualization, Funding acquisition, Resources, Writing – original draft, Writing – review & editing. **Norbert Marwan:** Conceptualization, Formal analysis, Funding acquisition, Validation, Writing – original draft, Writing – review & editing. **Frank Schaebitz:** Writing – review & editing. **Wolfgang Schwanghart:** Funding acquisition, Writing – original draft, Writing – review & editing. **Martin H. Trauth:** Conceptualization, Data curation, Formal analysis, Funding acquisition, Investigation, Methodology, Supervision, Validation, Visualization, Writing – original draft.

Declaration of competing interest

The authors declare that they have no known competing financial interests or personal relationships that could have appeared to influence the work reported in this paper.

Data availability

The data and analysis code will be available at GitHub and PANGAEA

Acknowledgments

Support for the Chew Bahir Drilling Project as part of the HSPDP has been provided by the International Continental Drilling Program (ICDP), the National Science Foundation (NSF), the UK Natural Environment Research Council, and the Germany Research Foundation (DFG). MLF has received financial support from Germany Research Foundation (DFG) grant TR 419/21 to MHT. Core KL 15 was collected during German R/V Meteor cruise 5 leg 2 in 1987 funded by the Germany Research Foundation (DFG) and Federal Ministry of Education and Research (BMBF). We thank Annett Junginger, Michael Hein, and Christian Schepers for their help, feedback, and fruitful discussions.

Appendix A. Supplementary data

Supplementary data to this article can be found online at https://doi.org/10.1016/j.qsa.2024.100174.

References

Ao, H., Ruan, J., Martinón-Torres, M., Krapp, M., Liebrand, D., Dekkers, M.J., Caley, T., Jonell, T.N., Zhu, Z., Huang, C., Li, X., Zhang, Z., Sun, Q., Yang, P., Jiang, J., Li, X., Xie, X., Song, Y., Qiang, X., et al., 2024. Concurrent Asian monsoon strengthening and early modern human dispersal to East Asia during the last interglacial. Proc. Natl. Acad. Sci. USA 121 (3), e2308994121. https://doi.org/10.1073/pnas.2308994121.

Aitchison, J., 1982. The statistical analysis of compositional data. J. Roy. Stat. Soc. B 44 (2), 139–160. https://doi.org/10.1111/j.2517-6161.1982.tb01195.x.

Almogi-Labina, A., Schmiedl, G., Hemleben, C., Siman-Tov, R., Segl, M., Meischner, D., 2000. The influence of the NE winter monsoon on productivity changes in the Gulf of Aden, NW Arabian Sea, during the last 530 ka as recorded by foraminifera. Mar. Micropaleontol. 40 (3), 295–319. https://doi.org/10.1016/s0377-8398(00)00043-8.

Armitage, S.J., Jasim, S.A., Marks, A.E., Parker, A.G., Usik, V.I., Uerpmann, H.-P., 2011. The southern route "out of Africa": evidence for an early expansion of modern humans into Arabia. Science 331 (6016), 453–456. https://doi.org/10.1126/science.1199113.

Asrat, A., Baker, A., Leng, M.J., Hellstrom, J., Mariethoz, G., Boomer, I., Yu, D., Jex, C.N., Gunn, J., 2018. Paleoclimate change in Ethiopia around the last interglacial derived from annually-resolved stalagmite evidence. Quat. Sci. Rev. 202, 197–210. https://doi.org/10.1016/j.quascirev.2018.06.016.

Beck, J.W., Zhou, W., Li, C., Wu, Z., White, L., Xian, F., Kong, X., An, Z., 2018. A 550,000-year record of East Asian monsoon rainfall from 10Be in loess. Science 360 (6391), 877–881. https://doi.org/10.1126/science.aam5825.

Bereiter, B., Eggleston, S., Schmitt, J., Nehrbass-Ahles, C., Stocker, T.F., Fischer, H., Kipfstuhl, S., Chappellaz, J., 2015. Revision of the EPICA Dome C CO2 record from 800 to 600 kyr before present. Geophys. Res. Lett. 42 (2), 542–549. https://doi.org/10.1002/2014gl061957.

Bergström, A., Stringer, C., Hajdinjak, M., Scerri, E.M.L., Skoglund, P., 2021. Origins of modern human ancestry. Nature 590 (7845), 229–237. https://doi.org/10.1038/s41586-021-03244-5.

Beyer, R.M., Krapp, M., Eriksson, A., Manica, A., 2021. Climatic windows for human migration out of Africa in the past 300,000 years. Nat. Commun. 12 (1) https://doi.org/10.1038/s41467-021-24779-1.

Blaauw, M., 2010. Methods and code for 'classical' age-modelling of radiocarbon sequences. Quat. Geochronol. 5 (5), 512–518. https://doi.org/10.1016/j.quageo.2010.01.002.

Breeze, P.S., Groucutt, H.S., Drake, N.A., White, T.S., Jennings, R.P., Petraglia, M.D., 2016. Palaeohydrological corridors for hominin dispersals in the Middle East ~250–70,000 years ago. Quat. Sci. Rev. 144, 155–185. https://doi.org/10.1016/j.quascirev.2016.05.012.

Bretzke, K., Preusser, F., Jasim, S., Miller, C., Preston, G., Raith, K., Underdown, S.J., Parton, A., Parker, A.G., 2022. Multiple phases of human occupation in Southeast Arabia between 210,000 and 120,000 years ago. Sci. Rep. 12 (1) https://doi.org/10.1038/s41598-022-05617-w.

Bretzke, Knut, Herkert, K., 2023. Jebel Faya and the middle to late Pleistocene transition: settlement continuity and behavioural flexibility. Paleorient 49 (1), 63–81. https://doi.org/10.4000/paleorient.2728.

Calvert, S.E., Pedersen, T.F., 2007. Chapter fourteen elemental proxies for palaeoclimatic and palaeoceanographic variability in marine sediments: interpretation and

application. Developments in Marine Geology 1, 567–644. https://doi.org/10.1016/s1572-5480(07)01019-6.
Carto, S.L., Weaver, A.J., Hetherington, R., Lam, Y., Wiebe, E.C., 2009. Out of Africa and into an ice age: on the role of global climate change in the late Pleistocene migration of early modern humans out of Africa. J. Hum. Evol. 56 (2), 139–151. https://doi.org/10.1016/j.jhevol.2008.09.004.
Castañeda, I.S., Mulitza, S., Schefuss, E., Lopes dos Santos, R.A., Sinninghe Damsté, J.S., Schouten, S., 2009. Wet phases in the Sahara/Sahel region and human migration patterns in North Africa. Proc. Natl. Acad. Sci. U.S.A. 106 (48), 20159–20163. https://doi.org/10.1073/pnas.0905771106.
Cember, R.P., 1988. On the sources, formation, and circulation of Red Sea deep water. J. Geophys. Res.: Oceans 93 (C7), 8175–8191. https://doi.org/10.1029/jc093ic07p08175.
Chan, E.K.F., Timmermann, A., Baldi, B.F., Moore, A.E., Lyons, R.J., Lee, S.-S., Kalsbeek, A.M.F., Petersen, D.C., Rautenbach, H., Förtsch, H.E.A., Bornman, M.S.R., Hayes, V.M., 2019. Human origins in a southern African palaeo-wetland and first migrations. Nature 575 (7781), 185–189. https://doi.org/10.1038/s41586-019-1714-1.
Claussen, M., Gayler, V., 1997. The greening of the Sahara during the mid-holocene: results of an interactive atmosphere-biome model. Global Ecol. Biogeogr. Lett. 6 (5), 369. https://doi.org/10.2307/2997337.
Clement, A.C., Hall, A., Broccoli, A.J., 2004. The importance of precessional signals in the tropical climate. Clim. Dynam. 22 (4), 327–341. https://doi.org/10.1007/s00382-003-0375-8.
Coetzee, J.A., 1964. Evidence for a considerable depression of the vegetation belts during the upper Pleistocene on the East African mountains. Nature 204 (4958), 564–566. https://doi.org/10.1038/204564a0.
Cohen, A., Campisano, C., Arrowsmith, R., Asrat, A., Behrensmeyer, A.K., Deino, A., Feibel, C., Hill, A., Johnson, R., Kingston, J., Lamb, H., Lowenstein, T., Noren, A., Olago, D., Owen, R.B., Potts, R., Reed, K., Renaut, R., Schäbitz, F., et al., 2016. The Hominin Sites and Paleolakes Drilling Project: inferring the environmental context of human evolution from eastern African rift lake deposits. Sci. Drill. 21, 1–16. https://doi.org/10.5194/sd-21-1-2016.
Drake, N.A., Blench, R.M., Armitage, S.J., Bristow, C.S., White, K.H., 2011. Ancient watercourses and biogeography of the Sahara explain the peopling of the desert. Proc. Natl. Acad. Sci. USA 108 (2), 458–462. https://doi.org/10.1073/pnas.1012231108.
Ehrmann, W., Wilson, P.A., Arz, H.W., Schulz, H., Schmiedl, G., 2024. Monsoon-driven changes in aeolian and fluvial sediment input to the central Red Sea recorded throughout the last 200 000 years. Clim. Past 20 (1), 37–52.
Emeis, K.C., Robertson, A.H.F., Richter, C., et al., 1996. Proceedings of the ocean drilling Program, 160 initial reports. In: Proceedings of the Ocean Drilling Program. https://doi.org/10.2973/odp.proc.ir.160.1996.
Faith, J.T., Du, A., Behrensmeyer, A.K., Davies, B., Patterson, D.B., Rowan, J., Wood, B., 2021. Rethinking the ecological drivers of hominin evolution. Trends Ecol. Evol. 36 (9), 797–807. https://doi.org/10.1016/j.tree.2021.04.011.
Fischer, M.L., Bachofer, F., Yost, C.L., Bludau, I.J.E., Schepers, C., Foerster, V., Lamb, H., Schäbitz, F., Asrat, A., Trauth, M.H., Junginger, A., 2021. A phytolith supported biosphere-hydrosphere predictive model for southern Ethiopia: insights into paleoenvironmental changes and human landscape preferences since the last glacial maximum. Geosciences 11 (10), 418. https://doi.org/10.3390/geosciences11100418.
Fleitmann, D., 1997. *Klastischer Eintrag in das Rote Meer und den Golf von Aden durch den Arabischen Monsun: Untersuchungen an Kolbenlot-Kernen.* Master's thesis Diplom-Arbeit. Institut und Museum für Geologie und Paläontologie der Georg-August-Universität zu Göttingen.
Foerster, V., Junginger, A., Landkamp, O., Gebru, T., Asrat, A., Umer, M., Lamb, H.F., Wennrich, V., Rethemeyer, J., N, N., Trauth, M.H., Schaebitz, F., 2012. Climatic change recorded in the sediments of the Chew Bahir basin, southern Ethiopia, during the last 45,000 years. Quat. Int. 274, 25. https://doi.org/10.1016/j.quaint.2012.06.028.
Foerster, Verena, Asrat, A., Ramsey, C.B., Brown, E.T., Chapot, M.S., Deino, A., Duesing, W., Grove, M., Hahn, A., Junginger, A., Kaboth-Bahr, S., Lane, C.S., Opitz, S., Noren, A., Roberts, H.M., Stockhecke, M., Tiedemann, R., Vidal, C.M., Vogelsang, R., et al., 2022. Pleistocene climate variability in eastern Africa influenced hominin evolution. Nat. Geosci. 15 (10), 805–811. https://doi.org/10.1038/s41561-022-01032-y.
Foerster, Verena, Deocampo, D.M., Asrat, A., Günter, C., Junginger, A., Krämer, K.H., Stroncik, N.A., Trauth, M.H., 2018. Towards an understanding of climate proxy formation in the Chew Bahir basin, southern Ethiopian Rift. Palaeogeogr. Palaeoclimatol. Palaeoecol. 501, 111–123. https://doi.org/10.1016/j.palaeo.2018.04.009.
Gebregiorgis, D., Deocampo, D.M., Foerster, V., Longstaffe, F.J., Delaney, J.S., Schaebitz, F., Junginger, A., Markowska, M., Opitz, S., Trauth, M.H., Lamb, H.F., Asrat, A., 2021. Modern sedimentation and authigenic mineral formation in the Chew Bahir basin, southern Ethiopia: implications for interpretation of late quaternary paleoclimate records. Front. Earth Sci. 9, 607695 https://doi.org/10.3389/feart.2021.607695.
Gosling, W.D., Scerri, E.M.L., Kaboth-Bahr, S., 2022. The Climate and Vegetation Backdrop to Hominin Evolution in Africa, 377. Philosophical Transactions of the Royal Society B: Biological Sciences. https://doi.org/10.1098/rstb.2020.0483, 1849.
Grant, K.M., Rohling, E.J., Westerhold, T., Zabel, M., Heslop, D., Konijnendijk, T., Lourens, L., 2017. A 3 million year index for North African humidity/aridity and the implication of potential pan-African Humid periods. Quat. Sci. Rev. 171, 100–118. https://doi.org/10.1016/j.quascirev.2017.07.005.
Groucutt, H.S., White, T.S., Scerri, E.M.L., Andrieux, E., Clark-Wilson, R., Breeze, P.S., Armitage, S.J., Stewart, M., Drake, N., Louys, J., Price, G.J., Duval, M., Parton, A., Candy, I., Carleton, W.C., Shipton, C., Jennings, R.P., Zahir, M., Blinkhorn, J., et al., 2021. Multiple hominin dispersals into Southwest Asia over the past 400,000 years. Nature. https://doi.org/10.1038/s41586-021-03863-y.
Groucutt, Huw S., Grün, R., Zalmout, I.A.S., Drake, N.A., Armitage, S.J., Candy, I., Clark-Wilson, R., Louys, J., Breeze, P.S., Duval, M., Buck, L.T., Kivell, T.L., Pomeroy, E., Stephens, N.B., Stock, J.T., Stewart, M., Price, G.J., Kinsley, L., Sung, W.W., et al., 2018. Homo sapiens in Arabia by 85,000 years ago. Nature Ecology & Evolution 2 (5), 800–809. https://doi.org/10.1038/s41559-018-0518-2.
Grove, M., 2014. Evolution and dispersal under climatic instability: a simple evolutionary algorithm. Adapt. Behav. 22 (4), 235–254. https://doi.org/10.1177/1059712314533573.
Hopley, P. J. & Maxwell, S. J. (n.d.). Environmental and stratigraphic bias in the Hominin Fossil Record: implications for theories of the climatic forcing of human evolution. In ["S.C. Reynolds and R. Bobe"] (Ed.), African Paleoecology and Human Evolution (pp. 15–23). Cambridge University Press. https://eprints.bbk.ac.uk/id/eprint/48443/.
Herbert, T.D., Peterson, L.C., Lawrence, K.T., Liu, Z., 2010. Tropical Ocean temperatures over the past 3.5 million years. Science 328 (5985), 1530–1534. https://doi.org/10.1126/science.1185435.
Hublin, J.J., Ben-Ncer, A., Bailey, S.E., Freidline, S.E., Neubauer, S., Skinner, M.M., Bergmann, I., Cabec, A.L., Benazzi, S., Harvati, K., Gunz, P., 2017. New fossils from Jebel Irhoud, Morocco and the pan-African origin of Homo sapiens. Nature 546 (7657), 289–292. https://doi.org/10.1038/nature22336.
Jimenez-Espejo, F.J., Martinez-Ruiz, F., Rogerson, M., González-Donoso, J.M., Romero, O.E., Linares, D., Sakamoto, T., Gallego-Torres, D., Ruiz, J.L.R., Ortega-Huertas, M., Claros, J.A.P., 2008. Detrital input, productivity fluctuations, and water mass circulation in the westernmost Mediterranean Sea since the Last Glacial Maximum. G-cubed 9 (11). https://doi.org/10.1029/2008gc002096 n/a-n/a.
Kaboth-Bahr, S., Gosling, W.D., Vogelsang, R., Bahr, A., Scerri, E.M.L., Asrat, A., Cohen, A.S., Düsing, W., Foerster, V., Lamb, H.F., Maslin, M.A., Roberts, H.M., Schäbitz, F., Trauth, M.H., 2021. Paleo-ENSO influence on African environments and early modern humans. Proc. Natl. Acad. Sci. USA 118 (23), e2018277118. https://doi.org/10.1073/pnas.2018277118.
King, G., Bailey, G., 2006. Tectonics and human evolution. Antiquity 80 (308), 265–286. https://doi.org/10.1017/s0003598x00093613.
Konijnendijk, T.Y.M., Ziegler, M., Lourens, L.J., 2014. Chronological constraints on Pleistocene sapropel depositions from high-resolution geochemical records of ODP Sites 967 and 968. Newsl. Stratigr. 47 (3), 263–282. https://doi.org/10.1127/0078-0421/2014/0047.
Kuper, R., Kröpelin, S., 2006. Climate-controlled holocene occupation in the Sahara: motor of africa's evolution. Science 313 (5788), 803–807. https://doi.org/10.1126/science.1130989.
Kutzbach, J.E., Guan, J., He, F., Cohen, A.S., Orland, I.J., Chen, G., 2020. African climate response to orbital and glacial forcing in 140,000-y simulation with implications for early modern human environments. Proc. Natl. Acad. Sci. U.S.A. 117 (5), 2255–2264. https://doi.org/10.1073/pnas.1917673117.
Kutzbach, J.E., Street-Perrott, F.A., 1985. Milankovitch forcing of fluctuations in the level of tropical lakes from 18 to 0 kyr. Nature 317 (6033), 130–134. https://doi.org/10.1038/317130a0.
Larrasoaña, J.C., Roberts, A.P., Rohling, E.J., Winklhofer, M., Wehausen, R., 2003. Three million years of monsoon variability over the northern Sahara. Clim. Dynam. 21 (7–8), 689–698. https://doi.org/10.1007/s00382-003-0355-z.
Laskar, J., Robutel, P., Joutel, F., Gastineau, M., Correia, A.C.M., Levrard, B., 2004. A long-term numerical solution for the insolation quantities of the Earth. Astron. Astrophys. 428 (1), 261–285. https://doi.org/10.1051/0004-6361:20041335.
Lawler, A., 2014. In search of green Arabia. Science 345 (6200), 994–997. https://doi.org/10.1126/science.345.6200.994.
Lisiecki, L.E., Raymo, M.E., 2005. A Pliocene-Pleistocene stack of 57 globally distributed benthic δ18O records. Paleoceanography 20 (1). https://doi.org/10.1029/2004pa001071 n/a-n/a.
Marwan, N., Donges, J.F., Donner, R.V., Eroglu, D., 2021. Nonlinear time series analysis of palaeoclimate proxy records. Quat. Sci. Rev. 274 https://doi.org/10.1016/j.quascirev.2021.107245.
Marwan, N., Romano, M.C., Thiel, M., Kurths, J., 2007. Recurrence plots for the analysis of complex systems. Phys. Rep. 438 (5–6), 237–329. https://doi.org/10.1016/j.physrep.2006.11.001.
Maslin, M.A., Brierley, C.M., Milner, A.M., Shultz, S., Trauth, M.H., Wilson, K.E., 2014. East African climate pulses and early human evolution. Quat. Sci. Rev. 101, 1–17. https://doi.org/10.1016/j.quascirev.2014.06.012.
Maslin, M.A., Shultz, S., Trauth, M.H., 2015. A synthesis of the theories and concepts of early human evolution. Phil. Trans. Biol. Sci. 370 (1663), 20140064 https://doi.org/10.1098/rstb.2014.0064.
Maslin, M.A., Trauth, M.H., 2009. Plio-Pleistocene East African Pulsed Climate Variability and its Influence on Early Human Evolution. The First Humans–Origin and Early Evolution of the Genus Homo, pp. 151–158.
McCave, I.N., Hall, I.R., 2006. Size sorting in marine muds: processes, pitfalls, and prospects for paleoflow-speed proxies. G-cubed 7 (10). https://doi.org/10.1029/2006gc001284.
McDougall, I., Brown, F.H., Fleagle, J.G., 2005. Stratigraphic placement and age of modern humans from Kibish, Ethiopia. Nature 433 (7027), 733–736. https://doi.org/10.1038/nature03258.
Mesa-Fernández, J.M., Martínez-Ruiz, F., Rodrigo-Gámiz, M., Jiménez-Espejo, F.J., García, M., Sierro, F.J., 2022. Paleocirculation and paleoclimate conditions in the western Mediterranean basins over the last deglaciation: new insights from sediment

composition variations. Global Planet. Change 209, 103732. https://doi.org/10.1016/j.gloplacha.2021.103732.
Nellen, W., Bettac, W., Roether, W., Schnack, D., Thiel, H., Weikert, H., Zeitzschel, B., 1996. MINDIK, Reise Nr, 5, p. 2. *Januar 1987 - 24. September 1987, Band I*. Leitstelle METEOR, Institut für Meereskunde der Universität Hamburg. https://www.tib.eu/de/suchen/id/awi%3Aae87e44d2e359b739019903d39da6bc86c462810.
Nicholson, Samuel L., Pike, A.W.G., Hosfield, R., Roberts, N., Sahy, D., Woodhead, J., Cheng, H., Edwards, R.L., Affolter, S., Leuenberger, M., Burns, S.J., Matter, A., Fleitmann, D., 2020. Pluvial periods in Southern Arabia over the last 1.1 million-years. Quat. Sci. Rev. 229 https://doi.org/10.1016/j.quascirev.2019.106112.
Otto-Bliesner, B.L., Russell, J.M., Clark, P.U., Liu, Z., Overpeck, J.T., Konecky, B., deMenocal, P., Nicholson, S.E., He, F., Lu, Z., 2014. Coherent changes of southeastern equatorial and northern African rainfall during the last deglaciation. Science 346 (6214), 1223–1227. https://doi.org/10.1126/science.1259531.
Packard, N.H., Crutchfield, J.P., Farmer, J.D., Shaw, R.S., 1980. Geometry from a time series. Phys. Rev. Lett. 45 (9), 712–716. https://doi.org/10.1103/physrevlett.45.712.
Palmer, P.I., Wainwright, C.M., Dong, B., Maidment, R.I., Wheeler, K.G., Gedney, N., Hickman, J.E., Madani, N., Folwell, S.S., Abdo, G., Allan, R.P., Black, E.C.L., Feng, L., Gudoshava, M., Haines, K., Huntingford, C., Kilavi, M., Lunt, M.F., Shaaban, A., Turner, A.G., 2023. Drivers and impacts of Eastern African rainfall variability. Nat. Rev. Earth Environ. 1–17. https://doi.org/10.1038/s43017-023-00397-x.
Parton, A., White, T.S., Parker, A.G., Breeze, P.S., Jennings, R., Groucutt, H.S., Petraglia, M.D., 2015. Orbital-scale climate variability in Arabia as a potential motor for human dispersals. Quat. Int. 382, 82–97. https://doi.org/10.1016/j.quaint.2015.01.005.
Pausata, F.S.R., Gaetani, M., Messori, G., Berg, A., Souza, D. M. de, Sage, R.F., deMenocal, P.B., 2020. The greening of the Sahara: past changes and future implications. One Earth 2 (3), 235–250. https://doi.org/10.1016/j.oneear.2020.03.002.
Petraglia, M.D., Parton, A., Groucutt, H.S., Alsharekh, A., 2015. Green Arabia: human prehistory at the crossroads of continents. Quat. Int. 382, 1–7. https://doi.org/10.1016/j.quaint.2015.05.071.
Potts, R., 1998. Variability selection in hominid evolution. Evol. Anthropol.: Issues, News, and Reviews: Issues, News, and Reviews 7 (3), 81–96.
Railsback, L.B., Gibbard, P.L., Head, M.J., Voarintsoa, N.R.G., Toucanne, S., 2015. An optimized scheme of lettered marine isotope substages for the last 1.0 million years, and the climatostratigraphic nature of isotope stages and substages. Quaternary Science Reviews 111, 94–106. https://doi.org/10.1016/j.quascirev.2015.01.012.
Reimer, P.J., Bard, E., Bayliss, A., Beck, J.W., Blackwell, P.G., Ramsey, C.B., Buck, C.E., Cheng, H., Edwards, R.L., Friedrich, M., Grootes, P.M., Guilderson, T.P., Haflidason, H., Hajdas, I., Hatté, C., Heaton, T.J., Hoffmann, D.L., Hogg, A.G., Hughen, K.A., et al., 2013. IntCal13 and Marine13 radiocarbon age calibration curves 0–50,000 Years cal BP. Radiocarbon 55 (4), 1869–1887. https://doi.org/10.2458/azu_js_rc.55.16947.
Roberts, H.M., Ramsey, C.B., Chapot, M.S., Deino, A.L., Lane, C.S., Vidal, C., Asrat, A., Cohen, A., Foerster, V., Lamb, H.F., Schäbitz, F., Trauth, M.H., Viehberg, F.A., 2021. Using multiple chronometers to establish a long, directly-dated lacustrine record: constraining >600,000 years of environmental change at Chew Bahir, Ethiopia. Quat. Sci. Rev. 266, 107025 https://doi.org/10.1016/j.quascirev.2021.107025.
Roberts, P., Prendergast, M.E., Janzen, A., Shipton, C., Blinkhorn, J., Zech, J., Crowther, A., Sawchuk, E.A., Stewart, M., Ndiema, E., 2020. Late Pleistocene to Holocene human palaeoecology in the tropical environments of coastal eastern Africa. Palaeogeogr. Palaeoclimatol. Palaeoecol. 537, 109438.
Rosenberg, T.M., Preusser, F., Fleitmann, D., Schwalb, A., Penkman, K., Schmid, T.W., Al-Shanti, M.A., Kadi, K., Matter, A., 2011. Humid periods in southern Arabia: Windows of opportunity for modern human dispersal. *Geology 39* (12), 1115–1118. https://doi.org/10.1130/g32281.1.
Sahle, Y., Morgan, L.E., Braun, D.R., Atnafu, B., Hutchings, W.K., 2014. Chronological and behavioral contexts of the earliest middle stone age in the Gademotta formation, main Ethiopian rift. Quat. Int. 331, 6–19. https://doi.org/10.1016/j.quaint.2013.03.010.
Scerri, E.M.L., Chikhi, L., Thomas, M.G., 2019. Beyond multiregional and simple out-of-Africa models of human evolution. Nature Ecology & Evolution 3 (10), 1370–1372. https://doi.org/10.1038/s41559-019-0992-1.
Scerri, E.M.L., Frouin, M., Breeze, P.S., Armitage, S.J., Candy, I., Groucutt, H.S., Drake, N., Parton, A., White, T.S., Alsharekh, A.M., Petraglia, M.D., 2021. The expansion of acheulean hominins into the nefud desert of Arabia. Sci. Rep. 11 (1) https://doi.org/10.1038/s41598-021-89489-6.
Scerri, E.M.L., Thomas, M.G., Manica, A., Gunz, P., Stock, J.T., Stringer, C., Grove, M., Groucutt, H.S., Timmermann, A., Rightmire, G.P., d'Errico, F., Tryon, C.A., Drake, N. A., Brooks, A.S., Dennell, R.W., Durbin, R., Henn, B.M., Lee-Thorp, J., deMenocal, P., et al., 2018. Did our species evolve in subdivided populations across Africa, and why does it matter? Trends Ecol. Evol. 33 (8), 582–594. https://doi.org/10.1016/j.tree.2018.05.005.
Schaebitz, F., Asrat, A., Lamb, H.F., Cohen, A.S., Foerster, V., Duesing, W., Kaboth-Bahr, S., Opitz, S., Viehberg, F.A., Vogelsang, R., Dean, J., Leng, M.J., Junginger, A., Ramsey, C.B., Chapot, M.S., Deino, A., Lane, C.S., Roberts, H.M., Vidal, C., et al., 2021. Hydroclimate changes in eastern Africa over the past 200,000 years may have influenced early human dispersal. Communications Earth & Environment 2 (1). https://doi.org/10.1038/s43247-021-00195-7.
Southon, J., Kashgarian, M., Fontugne, M., Metivier, B., Yim, W.W.-S., 2002. Marine reservoir corrections for the Indian ocean and southeast Asia. Radiocarbon 44 (1), 167–180. https://doi.org/10.1017/s0033822200064778.
Spearman, C., 1904. The proof and measurement of association between two things. Am. J. Psychol. 15 (1), 72. https://doi.org/10.2307/1412159. JSTOR.
Stein, M., Almogi-Labin, A., Goldstein, S.L., Hemleben, C., Starinsky, A., 2007. Late Quaternary changes in desert dust inputs to the Red Sea and Gulf of Aden from 87Sr/86Sr ratios in deep-sea cores. Earth Planet Sci. Lett. 261 (1–2), 104–119. https://doi.org/10.1016/j.epsl.2007.06.008.
Stewart, J.R., Fenberg, P.B., 2018. A climatic context for the out-of-Africa migration: comment. Geology 46 (5), e442. https://doi.org/10.1130/g40057c.1 e442.
Tierney, J.E., deMenocal, P.B., Zander, P.D., 2017. A climatic context for the out-of-Africa migration. Geology 45 (11), 1023–1026. https://doi.org/10.1130/g39457.1.
Timmermann, A., Friedrich, T., 2016. Late Pleistocene climate drivers of early human migration. Nature 538 (7623), 92–95. https://doi.org/10.1038/nature19365.
Tobler, R., Souilmi, Y., Huber, C.D., Bean, N., Turney, C.S.M., Grey, S.T., Cooper, A., 2023. The role of genetic selection and climatic factors in the dispersal of anatomically modern humans out of Africa. Proc. Natl. Acad. Sci. USA 120 (22), e2213061120. https://doi.org/10.1073/pnas.2213061120.
Trauth, M., Fischer, M. L., Foerster, V., Marwan, N., Roberts, H. M. & Schäbitz, F. (Submitted). A combined directly-dated and tuned age model for the Chew Bahir, Ethiopia. Quat. Sci. Rev..
Trauth, M.H., Asrat, A., Berner, N., Bibi, F., Foerster, V., Grove, M., Kaboth-Bahr, S., Maslin, M.A., Mudelsee, M., Schäbitz, F., 2021a. Northern hemisphere glaciation, African climate and human evolution. Quat. Sci. Rev. 268 https://doi.org/10.1016/j.quascirev.2021.107095.
Trauth, M.H., Asrat, A., Cohen, A.S., Duesing, W., Foerster, V., Kaboth-Bahr, S., Kraemer, K.H., Lamb, H.F., Marwan, N., Maslin, M.A., Schäbitz, F., 2021b. Recurring types of variability and transitions in the ~620 kyr record of climate change from the Chew Bahir basin, southern Ethiopia. Quat. Sci. Rev. 266 https://doi.org/10.1016/j.quascirev.2020.106777.
Trauth, M.H., Asrat, A., Duesing, W., Foerster, V., Kraemer, K.H., Marwan, N., Maslin, M. A., Schaebitz, F., 2019. Classifying past climate change in the Chew Bahir basin, southern Ethiopia, using recurrence quantification analysis. Clim. Dynam. 53 (5–6), 2557–2572. https://doi.org/10.1007/s00382-019-04641-3.
Trauth, M.H., Deino, A.L., Bergner, A.G.N., Strecker, M.R., 2003. East African climate change and orbital forcing during the last 175 kyr BP. Earth Planet Sci. Lett. 206 (3–4), 297–313. https://doi.org/10.1016/s0012-821x(02)01105-6.
Trauth, M.H., Maslin, M.A., Deino, A.L., Junginger, A., Lesoloyia, M., Odada, E.O., Olago, D.O., Olaka, L.A., Strecker, M.R., Tiedemann, R., 2010. Human evolution in a variable environment: the amplifier lakes of Eastern Africa. Quat. Sci. Rev. 29 (23–24), 2981–2988. https://doi.org/10.1016/j.quascirev.2010.07.007.
Trauth, M.H., Maslin, M.A., Deino, A., Strecker, M.R., 2005. Late cenozoic moisture history of East Africa. Science 309 (5743), 2051–2053. https://doi.org/10.1126/science.1112964.
Verschuren, D., Damsté, J.S.S., Moernaut, J., Kristen, I., Blaauw, M., Fagot, M., Haug, G. H., Geel, B. van, Batist, M.D., Barker, P., Vuille, M., Conley, D.J., Olago, D.O., Milne, I., Plessen, B., Eggermont, H., Wolff, C., Hurrell, E., Ossebaar, J., et al., 2009. Half-precessional dynamics of monsoon rainfall near the East African Equator. Nature 462 (7273), 637–641. https://doi.org/10.1038/nature08520.
Vidal, C.M., Lane, C.S., Asrat, A., Barfod, D.N., Mark, D.F., Tomlinson, E.L., Tadesse, A.Z., Yirgu, G., Deino, A., Hutchison, W., Mounier, A., Oppenheimer, C., 2022. Age of the oldest known Homo sapiens from eastern Africa. Nature 601 (7894), 579–583. https://doi.org/10.1038/s41586-021-04275-8.
Ward, J.H., 1963. Hierarchical grouping to optimize an objective function. J. Am. Stat. Assoc. 58 (301), 236–244. https://doi.org/10.1080/01621459.1963.10500845.
White, T.D., Asfaw, B., DeGusta, D., Gilbert, H., Richards, G.D., Suwa, G., Howell, F.C., 2003. Pleistocene Homo sapiens from middle awash, Ethiopia. Nature 423 (6941), 742–747. https://doi.org/10.1038/nature01669.
Ziegler, M., Jilbert, T., Lange, G. J. de, Lourens, L.J., Reichart, G., 2008. Bromine counts from XRF scanning as an estimate of the marine organic carbon content of sediment cores. G-cubed 9 (5). https://doi.org/10.1029/2007gc00193 n/a-n/a.